Semi-transparent SiC Schottky Diodes for X-ray spectroscopy

J.E. Lees*[1], D.J. Bassford[1], G.W. Fraser[1], A.B. Horsfall[2],
K.V. Vassilevski[2], N.G. Wright[2] and A. Owens[3]

Abstract

We describe a novel SiC Schottky diode architecture. The semi-transparent SiC Schottky diode has an “ultra-thin” (18 nm Ni/Ti) Schottky contact, a gold annular overlayer and a gold corner-contact pad. We show that the new architecture exhibits the same essential characteristics as a more conventional ‘thick-contact’ Schottky diode (≥ 100nm). Such diodes will have a higher efficiency for low energy (< 5 keV) X-rays than that of conventional structures combined with minimal self-fluorescence from the electrode materials. We present X-ray spectra from ^{55}Fe, ^{109}Cd and ^{241}Am radioactive sources that show these diodes can be used for spectroscopy with promising energy resolution (1.47 keV FWHM at 22 keV) at room temperature (23ºC). The reduction in contact thickness, however, does reduce the barrier height of the new diodes in comparison to those fabricated using the conventional process, and requires a trade-off between the low energy detection threshold and the noise in the detector.

PACS: 07.85.Fv, 29.40.Wk

Keywords: X-ray detection, Silicon Carbide, Schottky contact

*Corresponding author: +44 116 252 5519, E-mail address lee@star.le.ac.uk
[1]Space Research Centre, Department of Physics and Astronomy, Michael Atiyah Building, University of Leicester, Leicester, LE1 7RH, UK
[2] Semiconductor Technology Group, School of Electrical, Electronic and Computer Engineering, Merz Court, University of Newcastle, Newcastle, NE1 7RU, UK
[3]Office of Science Payload and Advanced Concepts, European Space Agency ESTEC SCI-A, Postbus 299, 2200AG Noordwijk, The Netherlands

1. Introduction

Silicon carbide (SiC) research has diversified enormously in recent years from its "traditional" base in power switching diodes into a wide range of applications such as trace gas sensing [1], UV detection [2], neutron counting [3], particle tracking [4], alpha particle detectors [5], X-ray analysis [6], and, recently, light ion detection [7]. New detectors based on this wide band gap semiconductor (E_g = 3.26 eV) could also find applications in areas such as biosensors [8] and small animal imaging as well as environmental monitoring. Future planetary landers and atmospheric probes will also require detectors to operate in harsh radiation environments and at room temperature or above [9].

Recently, Stroken et al. [10] have reported fabricating SiC transistors for use as α-particle detectors. The fabrication of signal level lateral transistor structures opens up the possibility of SiC imaging detectors with an advanced architecture similar to a silicon-based Active Pixel Sensor, but operable at room temperature or above without external cooling.

This paper describes the initial stages of a project to develop a radiation-hard [11] X-ray spectrometer capable of operation at high temperatures which matches the mission aims of ESA's Technology Reference Missions such as the *Venus Entry Probe (VEP)* [12] and *Jovian Minisat Explorer (JME)* [13].

For this application high quantum efficiency for photons with incident energies between 1 and 10 keV is essential. It is in this range where the elements Na (Z = 11, E_k = 1.04 keV) to Zn (Z = 30, E_k = 8.64 keV) have their K-shell emission lines. The need for high efficiency, low energy spectroscopy was the driving force behind the development of a new ultra-thin Schottky contact. We describe in Section 2 new "Semi-Transparent SiC Schottky Diodes (STSSD)", Section 3 describes the X-ray characterisation of the structures using laboratory and synchrotron sources.

2 Semi-transparent diode structure.

2.1 Fabrication

Semi-Transparent 4H-SiC Schottky Diodes were fabricated from commercial wafers produced by Cree Inc [14] that have a 20 μm epitaxial layer (doping concentration (N) of 4 x 10^{14} cm^{-3}) grown on a 370 μm substrate. After an RCA clean [15], a 25nm thick thermal oxide was grown to passivate the surface. A Ti/Ni based ohmic contact was deposited on the rear face of the substrate and annealed at 1100°C in vacuum. Windows were opened in this oxide using a buffered hydrofluoric acid etch, before deposition of 3nm of Ti and 12nm of Ni using e-beam evaporation. The samples were then annealed at 600°C to form NiSi, which has a greater thermal stability than pure Ni contacts. The overall thickness of the Schottky contact was estimated to be 18nm by means of step profilometry measurements. To facilitate wire bonding, 200nm thick gold bond pads were deposited on top of Cr adhesion layer in an annular arrangement. Figure 1 shows a schematic of the diode cross section, detailing the layers and structures, with their thicknesses and annealing temperatures.

Three different sizes of diode were fabricated: 180 x 180, 280 x 280 and 380 x 380 μm^2. Figure 2 shows the die layout and an optical image of one device.

The current voltage characteristics of the diode indicate that this new architecture exhibits an ideality factor and series resistance identical to those obtained for a traditional 'thick contact' device [16]. The ideality factor [17] was below 1.05, which is comparable to those for the thick contact device (1.04 - 1.06), indicating a high quality interface between the silicon carbide and the contact. Resistivities under forward conduction are close to 0.03 $Ohm.cm^2$ which are close to the resistivity of the epi-layer, demonstrating that the Schottky contact is continuous across the full area. However, the barrier height extracted from the forward characteristics by the modified Norde technique [18] is only 1.05eV, compared to the thick contact device, which has a barrier height of 1.45eV [16]. The reduced barrier height in comparison to a full thickness annealed Ti/Ni barrier is linked to the formation of a titanium rich alloy close to the SiC surface [19]. Whilst this reduction in barrier height increases the leakage current through the diode under reverse bias [17], the increase in practical diodes is lower than expected from theory due to the contributions from other conduction mechanisms including peripheral and surface leakage [20].

The reduction in the barrier height increases the FWHM noise in the system and so a compromise must be sought between the desire to observe low energy X-rays and the noise of the detection system, which has the possibility to swamp the region of interest.

2.2 X-ray absorption in the Schottky Contact

The ultra-thin Schottky contact (~18nm Ni/Ti) minimises the absorption in the electrode structure resulting in higher efficiencies (up to x100) for low energy X-rays (< 10 keV) compared to "standard" Schottky diode contact, Ni or Ti (contact thickness > 100nm). Figure 3 compares the calculated absorption [21, 22] of the Schottky metallization for the semi-transparent architecture and two Schottky diodes from the literature. The Schottky contact of Vittone et.al. [23] comprised 100 nm of gold (2mm in diameter) while the Schottky diode investigated by Nava et.al. [24] had a metallization layer of 200 nm Ni. It is clear from figure 3 that, as expected, the thinner Schottky contact has a much lower absorption and therefore one would predict higher detection efficiencies especially for X-ray energies below 10 keV.

2.3 I-V measurements

The I-V characteristics of diodes on two chip sets (fig. 2), designated 080102 and 090307, were measured using a calibrated Keithley 427 ammeter [25]. Two diodes, one from each chip set, were chosen for their low leakage current and were used to build (Leicester) two detectors, designated A (380 x 380 μm^2, STSSD 080102) and B (280 x 280 μm^2, STSSD 090307). Figure 4 shows the leakage current for these two diodes as a function of bias voltage over the range 0 to – 90V. Why the leakage current for the smaller diode (used in Detector B) should be higher at bias voltages greater than 50 Volts than that measured for the smaller diode is, at present, unknown. One possible cause could be the quality of the SiC wafer. The original SiC wafer did contain some defects however these areas were well mapped and were not used for diode fabrication.

The X-ray characterisation of Detector A was investigated in Leicester using radioactive sources whereas Detector B was characterised using the synchrotron source at HASYLAB and BESSY.

3. X-ray spectra

We measured the X-ray response of Detector A using three radioactive sources, ^{55}Fe, ^{109}Cd and ^{241}Am. Each source was placed in turn at a constant distance of approximately 3 cm above the diode under test.

The bias voltage used for the X-ray measurements (60V for ^{55}Fe and ^{109}Cd, 80V for ^{241}Am) was chosen as a good compromise between minimising the leakage current and matching the diode to input FET characteristics (leakage current and capacitance) while obtaining sufficient depletion depth (calculated to be ~12.7 μm at 60V and ~14.7 μm at 80V [26]). The accumulation time varied depending on the activity of the source.

3.1 ^{55}Fe X-ray spectra

Figure 5 shows a spectrum from Detector A operated at room temperature (23°C) illuminated by a (0.15 MBq) ^{55}Fe source. The energy threshold was set

to 3 keV by means of the input discriminator level of the MCA to reduce the number of noise events. The energy resolution for the peak at 5.9 keV was 1.5 keV Full Width at Half Maximum (FWHM) which is not sufficient to resolve the Mn K_α and K_β peaks (5.9 keV and 6.4 keV resp.) emitted by the ^{55}Fe source. Although the energy resolution is modest when, say, compared with a cooled CCD (130 eV) [27] we re-emphasis that this spectrum was taken at room temperature using an experimental type of diode.

Figure 5 also compares the measured spectrum with our spectroscopic model for SiC detectors which takes into account a wide range of physical parameters such as absorption, doping concentration, depletion depth and ambient temperature [28]. The parameters used in the model were 0.12 for the Fano factor, F, and 7.8eV for the electron-hole pair creation energy, w [29]. If the diode was Fano limited then the energy resolution would be 175 eV. Modelling of the measured FWHM in figure 5 shows that the electronic noise dominates and has an Electronic Equivalent Noise (ENC) of ~80 electrons (rms).

The STSSD was connected to a charge sensitive preamplifier which had a JFET (Vishay Siliconix 2N4416, capacitance ~2 pF [30]) as the input transistor. The STSSD capacitance values were 1.2 pF (detector A at 60 V bias) and 0.6 pF (detector B at 80 V bias) respectively. The output signal from the charge amplifier was modified by a shaping amplifier (Oretc 571 [31]). The variation of the ENC as a function of shaping amplifier time constant, without the diode attached, was assessed at room temperature following Bertuccio et al. [32]. Radioactive sources, ^{55}Fe and ^{109}Cd, were used as calibration sources. The minimum ENC, 44 electrons (rms), corresponded to a time constant of 3 μs.

The contribution to the total ENC from the SiC diode leakage current (1pA at 60 V) was estimated, for room temperature operation, to be ~5 electrons rms ([32] assuming $\alpha = 1$ and $A_3 = 2$). After subtracting (in quadrature) all the measured and calculated ENC contributions, the remaining contribution to the total ENC, 66 electrons rms, must therefore be due to the diode, its mounting materials and the overall diode-amplifier configuration.

We are currently investigating ways to reduce these noise sources to improve the energy resolution of our devices.

3.2 ^{109}Cd X-ray spectra

Figure 6 is a spectrum from a (1MBq) ^{109}Cd source, accumulated for ~72 hours. For these measurements the low energy threshold was set at 5 keV. The two Ag-K peaks, at 22.16 keV and 24.95 keV, are clearly resolved. The FWHM of the K_α.was estimated, by fitting it with a Gaussian distribution, to be 1.47 keV. The ^{109}Cd source is housed in a stainless steel capsule. The low energy shoulder and peak at ~ 6.5 keV we attribute to fluorescence of elements in the stainless steel capsule of the radioactive source, for example Fe-K (6.4 keV) and Ni-K (7.5 keV).

3.3 ^{241}Am X-ray spectra

Figure 7 is a spectrum from a (~70 MBq) ^{241}Am source, accumulated for ~142 hours. The long accumulation time was necessary to obtain sufficient events in the 59.5 keV peak to allow a statistically significant measure of the FWHM (1.7 keV). The ^{241}Am source had a 0.25 mm thick stainless steel window which essentially blocks all X-ray lines below 20 keV.

The low energy shoulder and peak, more evident than in fig. 6, we attribute to fluorescence in the stainless steel window.

3.4 Synchrotron source

X-ray characterisation of Detector B was investigated using beamline X1 (ROMO II) at HASYLAB [33] over the energy range 10 – 100 keV. The detector was mounted on an XY translation stage with a position resolution of 1 μm. An X-ray spot size of 10 μm x 10 μm was used to measure the characteristics of this diode. Detector B operated with a reverse bias of 80V during all synchrotron measurements

3.4.1 X-ray spectra

X-ray spectra were accumulated at discrete energies over the full available energy range. Figure 8 shows a representative spectrum taken at 60 keV. The Compton edge at ~11.3 keV is clearly distinguishable in the spectra measured at the synchrotron (Fig. 8), in comparison the low energy (<11 keV) of the spectrum measured using the ^{241}Am radioactive source (Fig. 7) is dominated by the fluorescence of elements in the same source (Section 3.3). The FWHM for the 60 keV peak is ~2.2 keV. This is greater than the measured FWHM at 60 keV, 1.7 keV, for Detector A (Fig. 7). This trend between the detectors is seen for all the measured energies, figure 9. The differences in energy resolution between the two diodes cannot be attributed to the difference of the diodes leakage currents and capacitances. Therefore the reasons are at present unknown but maybe due to small variations in the overall diode-amplifier configuration, environmental factors or localized variation in wafer quality. Both detector responses are proportional to ~1/E whereas for a Fano limited system the response would be proportional to ~1/$E^{0.5}$. Analysis of the measured FWHM (Section 3.1) shows that the electronic noise dominates, with an Electronic Equivalent Noise (ENC) of ~80 electrons (rms).

3.4.2 Uniformity

The uniformity of the Detector B was probed by traversing the monochromatic X-ray spot (10 μm x 10 μm) across the diode in 10 μm steps. The uniformity of the diode was assessed by measuring the peak X-ray energy response, at 12 keV, as a function of position, figure 10.This remarkable uniformity (<1%) is promising for the future production of small pixel arrays.

3.4.3 Linearity

Figure 11 shows the linearity of the two detectors as a function of energy. It is clear that the response is not linear over the measured range. The linearity of the signal amplifying chain (charge and shaping amplifiers) was investigated using a test pulse injected into the input FET via a ~1pF test capacitor. Figure 12 shows that the amplifying chain is linear over the range of our measurements. The three values corresponding to the X-ray peaks (5.9, 22.16 and 59.5 keV) from the radioactive source measurements have been included on the graph for comparison. It must be noted that although the STSSD was designed primarily as a low energy X-ray detector having a depletion layer of 15 microns, it can be viewed as a depleted region (15 microns) on top of a thick SiC substrate. The bias voltage is across the whole 390 microns (fig.1) thick SiC wafer so electrons created in the substrate region by high energy X-rays will still be collected at the readout electrode. This explains the increasing behaviour of the peak channel value with increasing X-ray energy reported in Fig.11. Indeed, while the photo-electrons associated with 60 and 100 keV X-rays (range 23 and 54 microns respectively [34]) loose only 17.2 keV and 12.5 keV in the 15 microns SiC diode [35], they will loose their total energy in the thick SiC substrate. From this we can assume that the measured nonlinearity could be due to charge loss or trapping in the SiC bulk. However, the measured data can be fitted with a polynomial (order 3) which could be used to correct for the non-linearity.

3.4.4 X-ray Efficiency

The X-ray efficiency of the STSSD (Detector B) was measured over the energy range 8 – 30 keV at BESSY II BAMline [36, 37]. A n-type Ge detector was used as the reference counter. Figure 13 shows the good agreement between the measured detector's efficiency and that calculated for a SiC diode with a depletion depth of ~14.7 μm and a doping concentration of $4x10^{14}$ cm^{-3} operated at 80V bias [26].

4. Discussion

The spectra reported in the previous sections show that the SiC Schottky diode is functioning as a good X-ray spectrometer with modest energy resolution over a wide energy range 3 – 100 keV.

There are a number of areas that require further development for SiC detectors to achieve operational characteristics (energy threshold ~1keV, energy resolution ≤5% @ 6 keV, imaging X-ray spectroscopy) closer to those required for a wide range of applications such as: remote sensing planetary missions, X-ray fluorescence spectroscopy in hazardous environments.

Improving the suitability of SiC diodes as X-ray detectors will require better quality SiC wafers. Major manufacturers, such as Cree and II-VI [14, 38] are improving the quality of commercial wafers. Recently Nakamura et al [39] have reported a new technique for growing essential defect free wafers using the “repeated a-face” growth process. This material is not, as yet, available

commercially but when available will undoubtedly lead to devices of much higher quality than are currently possible. Cree Inc, the dominant supplier of high quality silicon carbide material, have recently launched zero micropipe wafers, in which the micropipe (the dominant form of crystal fault) density is zero and this offers the possibility of a better yield for devices and opens up the possibility of pixellated arrays.

Acknowledgements

This research was supported by an RCUK Basic Technology Proof of Concept Grant “A detector for all seasons: towards Silicon Carbide imaging arrays” (EP/D004853/1). Part of this work was funded by the European Space Agency under contract (ESTEC 19382/05/NL/NR). The authors would also like to thank the station scientists Dr. Adam Webb, HASYLAB at DESY and Dr. Michael Krumrey, PTB Laboratories, BESSY-II.

References

[1]. A.B. Horsfall, et al., European Conference on Silicon Carbide and Related Materials, Newcastle upon Tyne, UK, 2006

[2]. Photonic Detectors Inc. 80-A West Cochran Street, Simi Valley, California, USA 93065

[3]. R.H. Ruddy et al., IEEE NSS-MIC conference, Rome 2004

[4]. M. Rogalla et al., Nuclear Physics B (Proc. Suppl.) 78 (1999) 516

[5]. A. Ivanov, et al., Materials Science Forum 483-485 (2005) 1029

[6]. G. Bertuccio et al., Nucl. Inst.Meth A 518 (2004) 433

[7]. M. De Napoli et al, Nucl. Inst. Meth. A 572 (2007) 831

[8]. P. Godignon, Material Science Forum 483-485 (2005) 1009

[9]. Owens et al., SPIE High-Energy Detectors in Astronomy 5501 (2004): 403.

[10]. N. B. Strokan et al., Semiconductors 37 (2003) 65

[11]. P.J. Sellin and J. Vaitkus, Nucl. Inst.Meth A 557 (2006) 479

[12]. *Venus Entry Probe:http://sci.esa.int/science-e/www/object/index.cfm?fobjectid=35987*

[13]. Jovian Minisat Explorer: http://sci.esa.int/science-e/www/object/index.cfm?fobjectid=35982

[14]. CREE Research Inc., 4600 Silicon Dive, Durham, NC 27703, USA

[15]. W. Kern and D.A. Puotien, RCA Review, 30 (1970) 187

[16]. K.V. Vassilevski et al., Materials Science Forum, 527-529 (2006) 931

[17]. C. Blasciuc-Dimitriu et al., Semiconductor Science and Technology, 20 (2005) 10

[18]. A.H. Norde, Journal of Applied Physics, 50 (1979) 5052

[19]. I.P. Nikitina, et al., Semiconductor Science and Technology, 21, (2006), 898

[20]. A.B. Horsfall, et al, Mat Sci Forum, 389 - 393 (2002), 1149

[21]. G.F. Knoll, Radiation detection and measurement, 3rd Ed. John Wiley and Sons, Inc., 2000, ISBN 0-471-07338-5

[22]. http://physics.nist.gov/PhysRefData/contents-xray.html

[23]. E. Vittone et al., Proceedings of the II workshop SiC, 18-19 March 2002, CNR-MASPEC, Parma.

[24]. F. Nava et al., Nucl. Inst. Meth. A 510 (2003) 273

[25]. Keithley Instruments Ltd, Unit 2 Commerce Park, Brunel Road, Theale, Berksire RG7 4AB, UK

[26]. R.H. Ruddy et al., IEEE Trans. Nucl. Sci. 45 (1998) 536

[27]. H. Nakajima et al., Nucl. Inst.Meth A 541 (2005) 365

[28]. J.E. Lees et al, in preparation.

[29]. G. Bertuccio and R. Casiraghi, IEEE Trans. Nucl. Sci. 50 (2006) 175

[30]. Vishay Intertechnology Inc., 62 Lancaster Avenue Malvern, PA 19355-2143, USA

[31]. Ortec, 801 South Illinois Avenue, Oak Ridge, TN 37830, USA

[32]. G. Bertuccio et al, Nuc. Inst. Meth. A 380 (1996) 301

[33]. HASYLAB at DESY, Notkestr. 85, D-22603 HAMBURG, Germany

[34]. ESTAR http://physics.nist.gov/PhysRefData/Star/Text/ESTAR.html

[35]. M.V. Zombeck, Handbook of Space Astronomy and Astrophysics, 3rd Ed. Cambridge University Press, 2007, ISBN-13 978-0-521-78242-5

[36]. Berliner Elektronenspeicherring-Gesellschaft für Synchrotronstrahlung m.b.H., Albert-Einstein-Str.1512489 Berlin, Germany.

[37]. M. Krumrey and G. Ulm, Nucl. Inst.Meth A 467-468, (2001) 1175

[38]. II-VI Inc., II-VI Wide Bandgap Group, 20 Chapin Road, Suite 1005, PO Box 840, Pine Brook, NJ 07058

[39]. D. Nakamura et al., Nature 430 (2004) 1009

Figures: J.E. Lees et al. Semi-transparent Schottky...

Figure 1

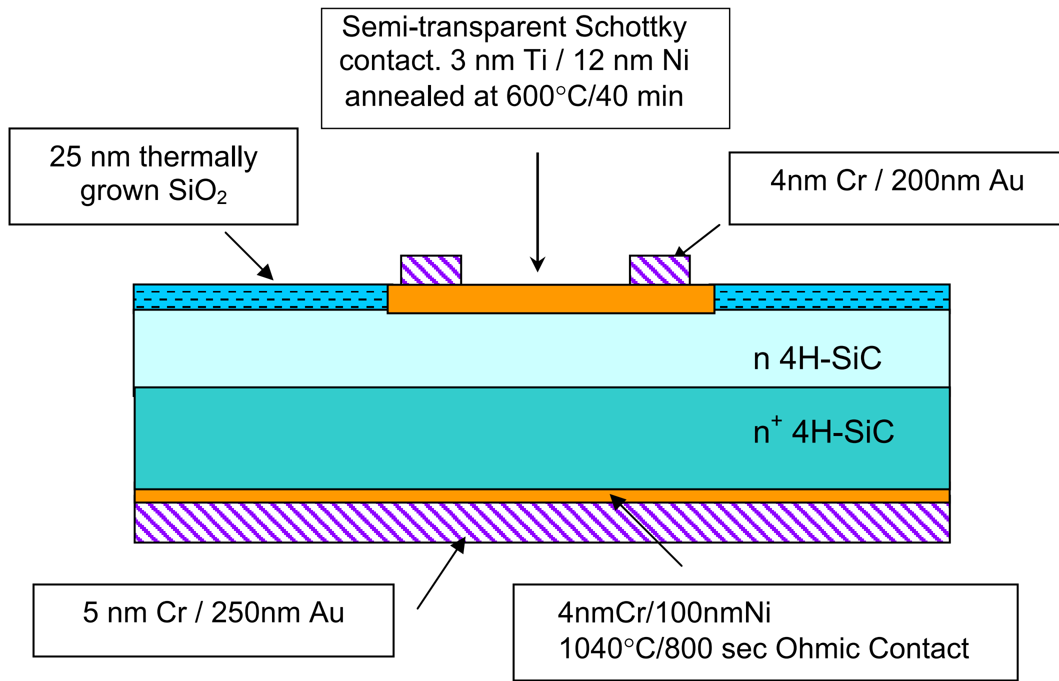

Figure 2

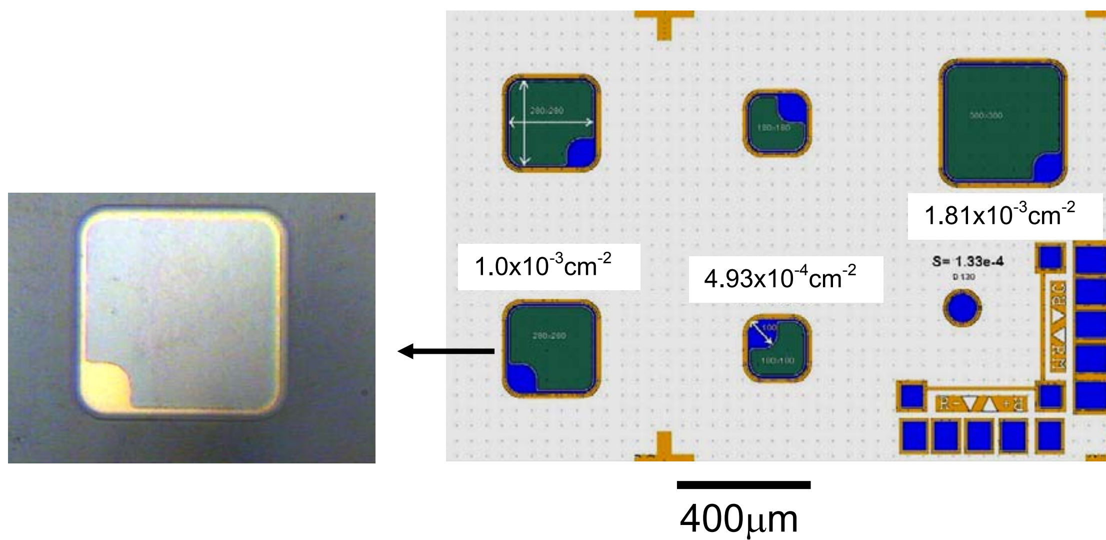

Figures: J.E. Lees et al. Semi-transparent Schottky...

Figure 3

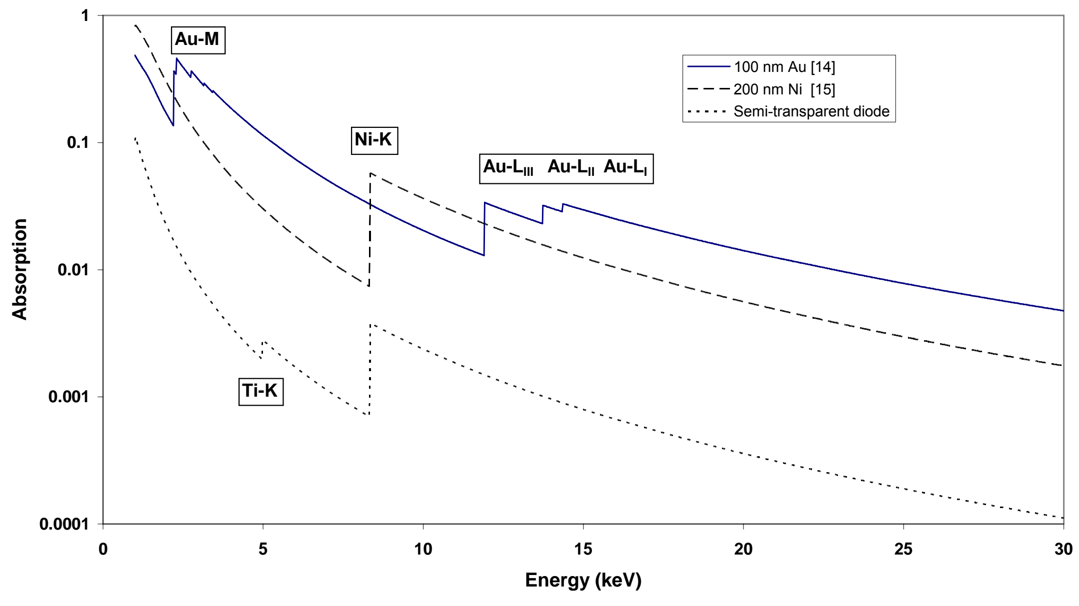

Figure 4

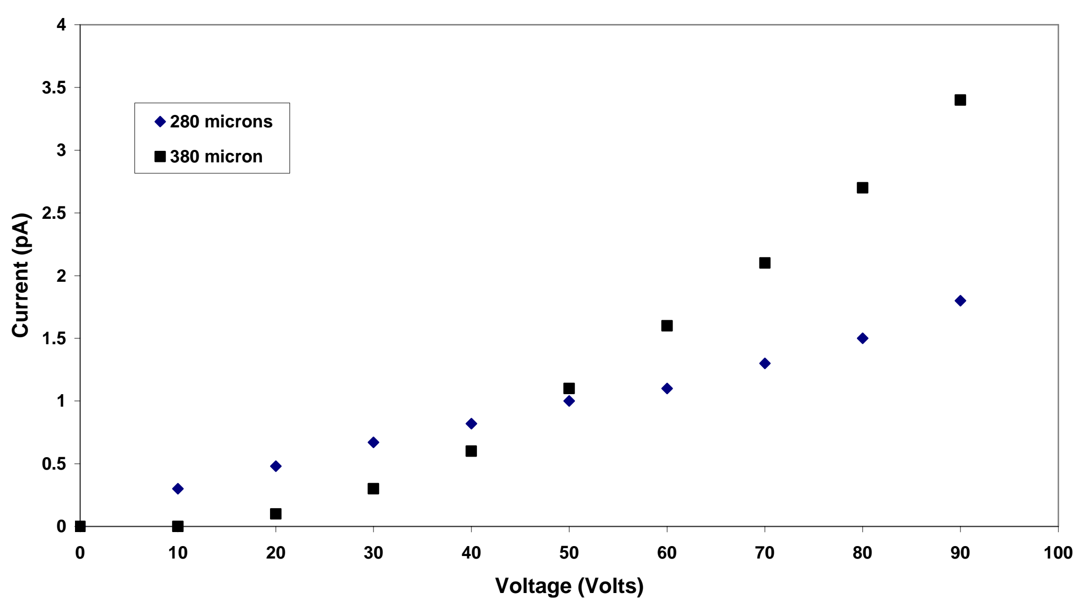

Figures: J.E. Lees et al. Semi-transparent Schottky...

Figure 5

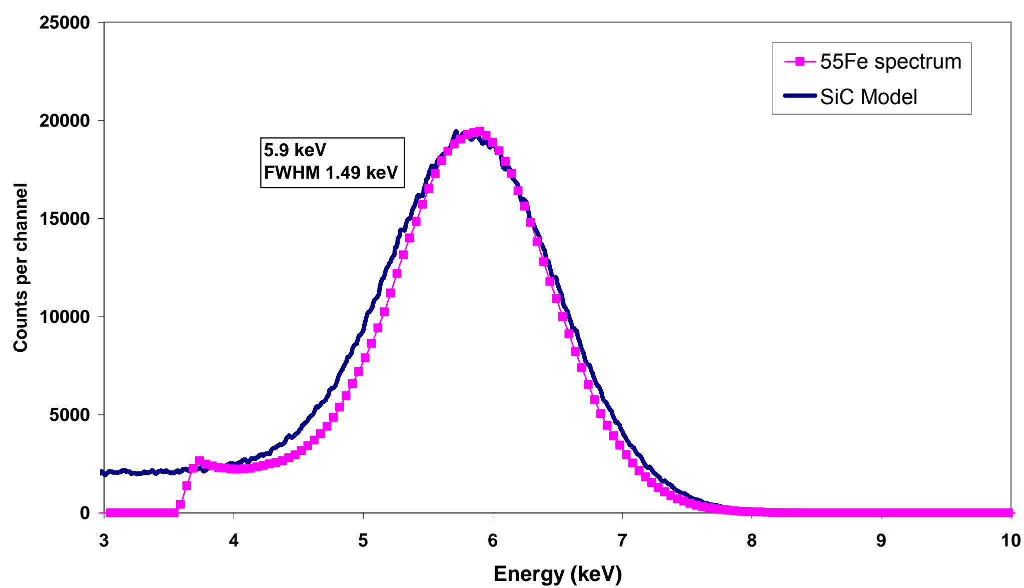

Figure 6

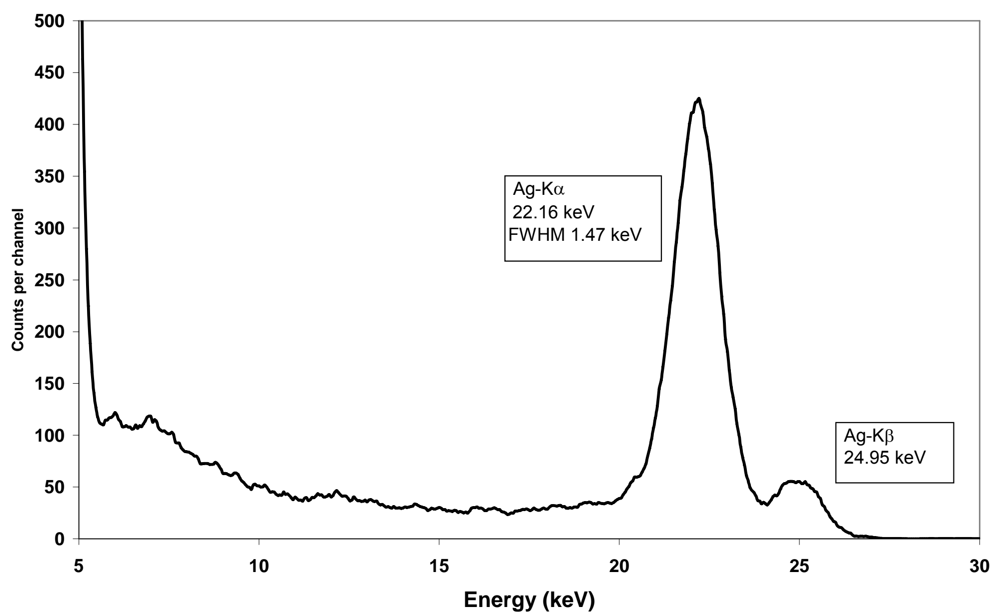

Figures: J.E. Lees et al. Semi-transparent Schottky...

Figure 7

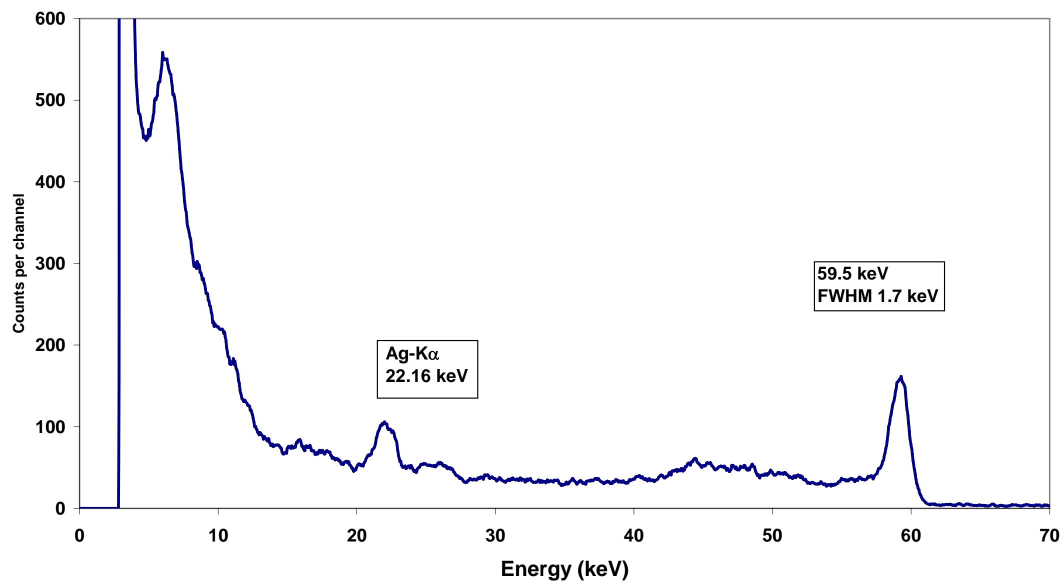

Figure 8

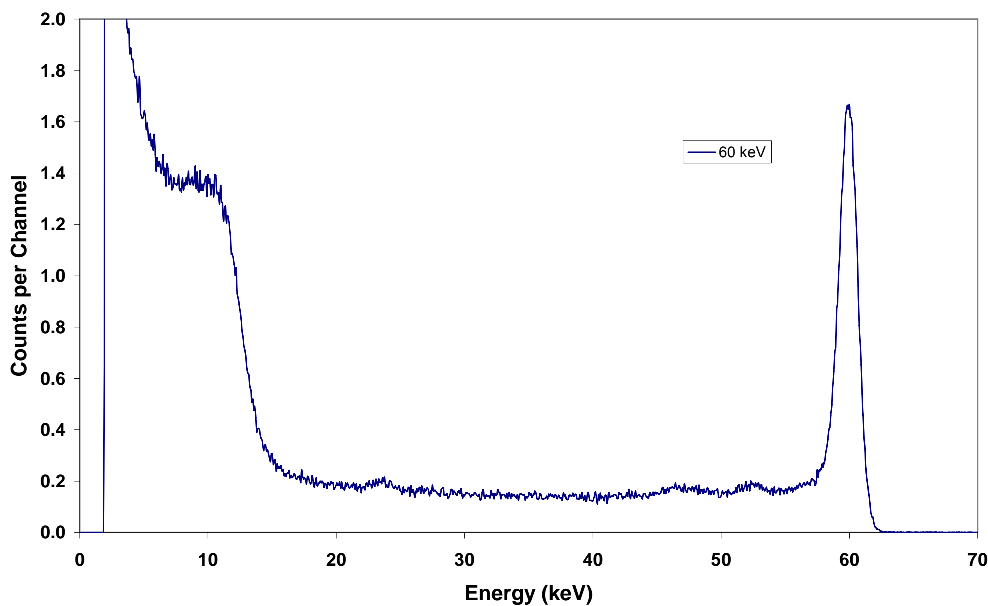

Figures: J.E. Lees et al. Semi-transparent Schottky...

Figure 9

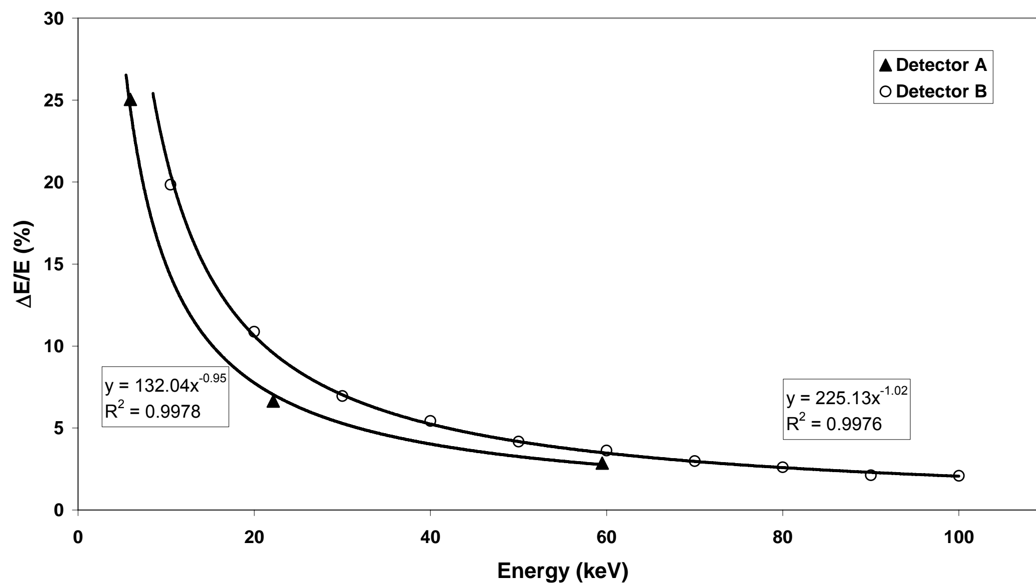

Figure 10

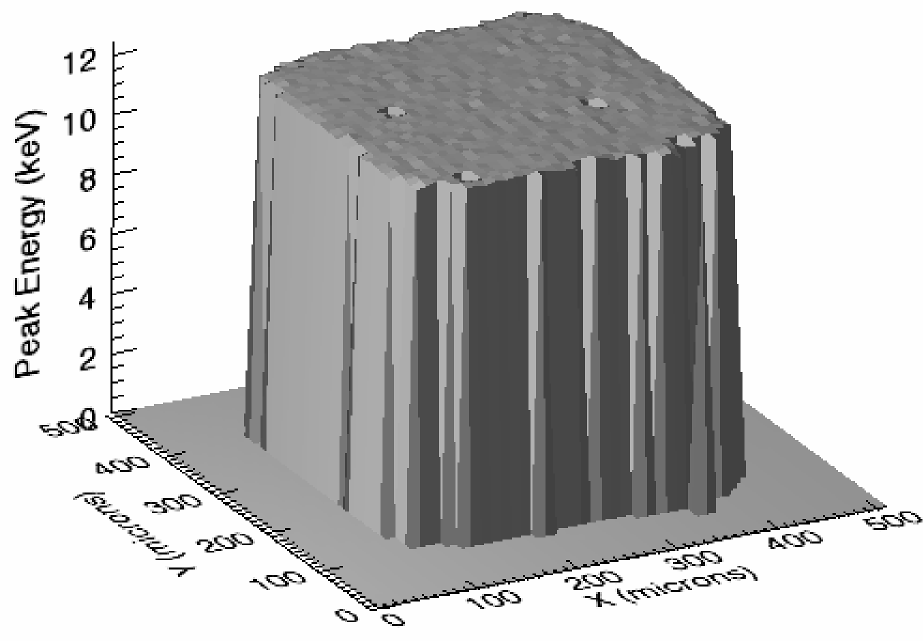

Figures: J.E. Lees et al. Semi-transparent Schottky...

Figure 11

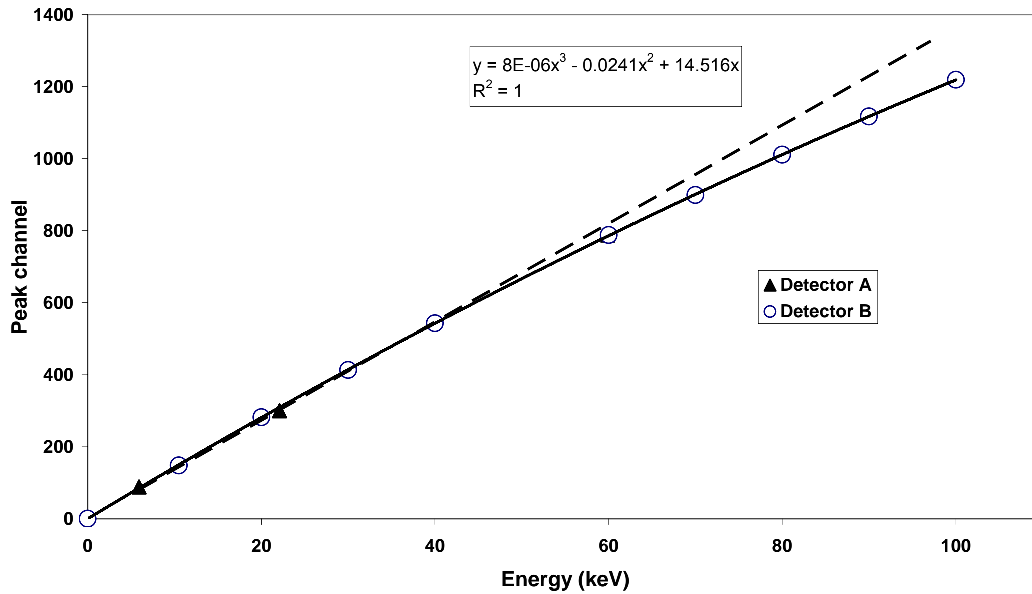

Figure 12

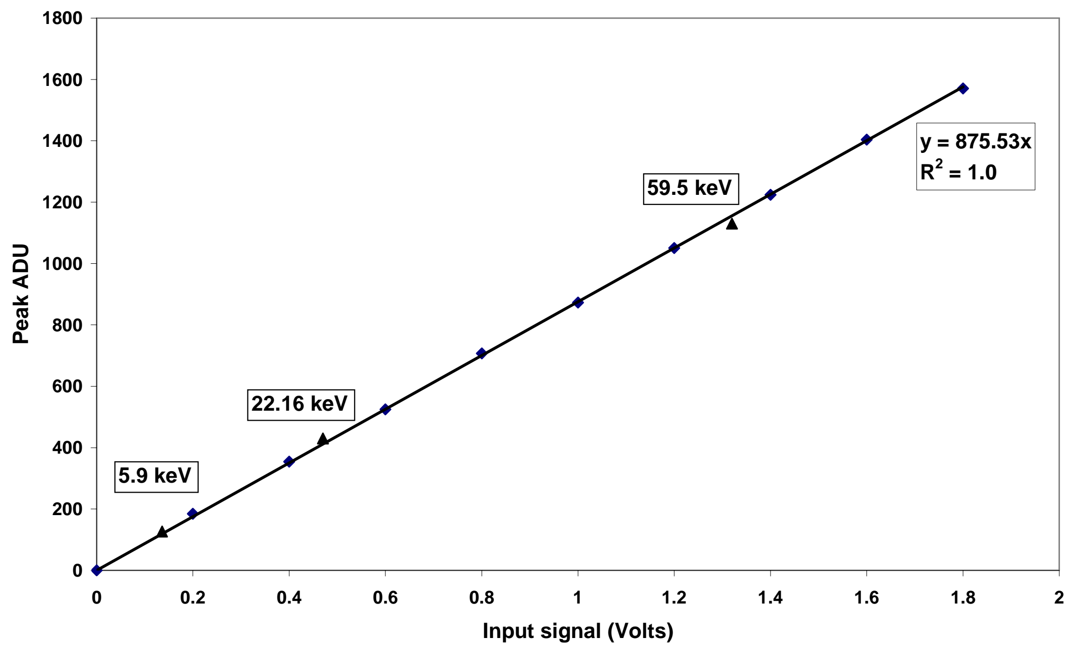

Figure 13

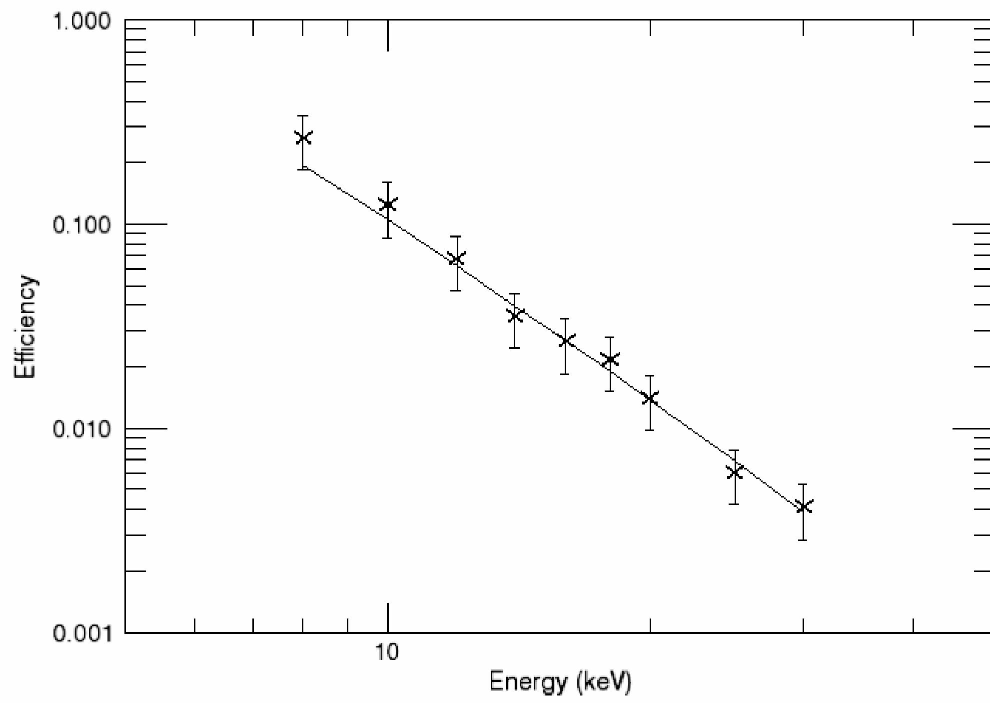

Figure Captions: J.E. Lees et al. Semi-transparent Schottky...

Fig. 1. Cross-section of 4H-SiC diode with semi-transparent Schottky contact (not to scale). Epitaxial thickness 20 microns and resistive n+ layer thickness of 370 microns

Fig. 2. Semi-Transparent SiC Schottky diodes. The right hand picture is a schematic of the die layout showing a range of diode sizes. The labels indicate the area of each diode. The left hand picture is an optical image of one STSSD (280×280 µm) showing the semi-transparent Schottky contact and gold bond pad and annular overlay.

Fig. 3 X-ray absorption versus energy in Schottky contacts of various thicknesses and compositions. The various material absorption edges are labelled.

Fig. 4 Current vs reverse bias voltage for the 280 and 380 μm STSSD.

Fig. 5 Comparison of a ^{55}Fe spectrum from the Semi Transparent SiC Schottky Diode (bias voltage 60V) with a SiC X-ray model [28]. Squares: measured spectra, solid line: model. Energy per channel is 50eV. The parameters used in the model were 0.12 for the Fano factor, 7.8eV for the electron-hole energy and an ENC of 80 electrons rms. Accumulation time for experimental spectrum: 17 hours.

Fig. 6. Spectrum from a ^{109}Cd source. Accumulation time: 17 hours. The Gaussian fit to the Ag-Kα peak is shown by the dotted curve.

Fig. 7. Spectrum from a ^{241}Am source, accumulated for ~142 hours. The primary X-ray peaks are labelled.

Fig. 8. The spectrum of Detector B illuminated with 60 keV X-rays, accumulated for ~26 minutes.

Fig. 9. Energy resolution for Detectors A (triangles) and B (open circles) as a function of energy. Each data set has been fitted by a power series with indices - 0.95 and – 1.02 for Detector A and B respectively.

Fig. 10. Gain uniformity of the STSSD illuminated by 12 keV X-rays.

Fig. 11. Peak channel as a function of energy. Triangles: Detector A, Open circles: Detector B. The solid line is a best fit using a polynomial order 3. The broken line indicates the response for a “perfectly” linear system.

Fig. 12. The linearity of Detector A amplifying chain. Diamonds: test pulses, Triangles: signal values corresponding to the X-ray peaks (5.9, 22.16 and 59.5 keV). The solid line is the best fit to the test pulse data set.

Fig. 13. X-ray efficiency as a function of energy for a STSSD (detector B). Crosses measured efficiencies, solid line: calculated efficiencies.